Annex A. Research Methodology of Gaseous Fuels and Fuel Injection Systems

A.1. Experimental Setup of Gaseous Fuel Research

Fig. A.1.1 shows prepared engine test bench for experimental investigation of petrol and biogas fuel mixtures.

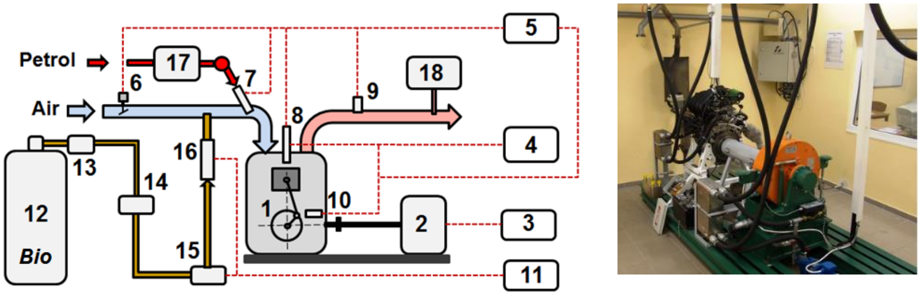

a) b)

Fig. A.1.1. Testing equipment for petrol and biogas fuel mixtures in spark ignition engine: a) schematic of engine stand testing equipment for petrol and biogas experimental investigation, b) test equipment in VGTU laboratory facilities

The experimental setup is explained from Fig. A.1.1 like that: 1 – SI engine *Nissan HR16DE*; 2 – engine load stand *AMX 200/100*; 3 – load stand electronic control unit; 4 – equipment for registration of pressure in the cylinder *AVL DiTEST DPM* 800; 5 – engine electronic control unit *MoTeC M800*; 6 – throttle control servo-motor; 7 – petrol injector; 8 – spark plug with integrated pressure sensor *AVL ZI31*; 9 – wideband oxygen sensor *Bosch LSU 4.9*; 10 – crankshaft position sensor; 11 – gas equipment control unit *OSCAR*–N; 12 – biogas (*Bio*) cylinder at 200 bar; 13 – high pressure reducer; 14 – gas flow meter *KG-0095-G06-94-10*; 15 – low pressure reducer; 16 – gas injector; 17 – petrol consumption metering device *AMX 212F*; 18 – exhaust gas analyser *AVL DiCom 4000*.

Table A.1. Injectors parameters of direct injection system

Fuel	Methane, natural gas
Mixture formation	DI, spray guided
Actuation type	Solenoid
Max fuel injection pressure, bar	18
Injector opening type	Outwards, A nozzle

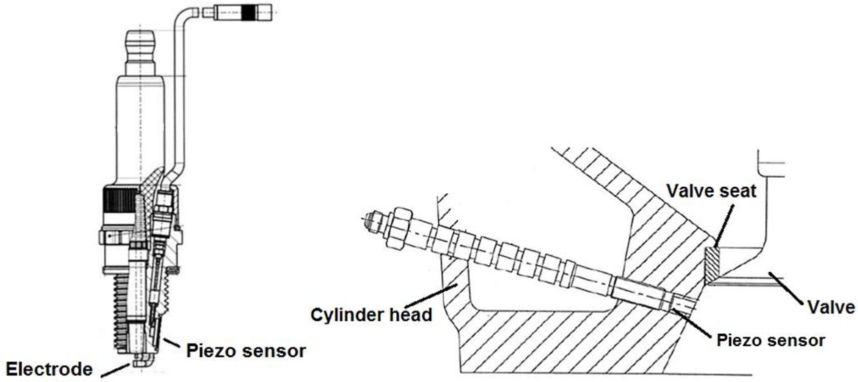

a) b)

Fig. A.1.2. Pressure sensors used in experiments: a) pressure sensor is mounted in a spark plug (AVL 2011); b) pressure sensor is mounted in a cylinder head (Kistler 2016)

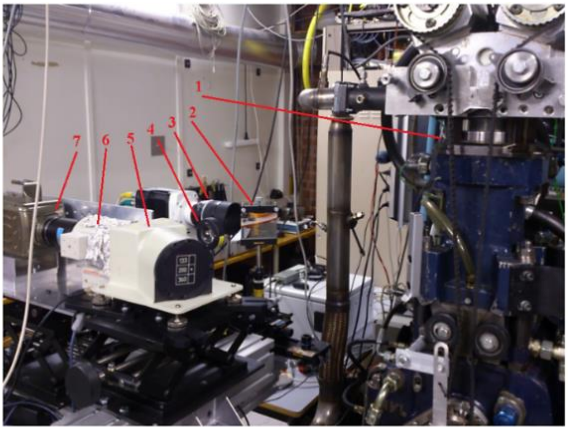

Fig. A.1.3. Experimental setup with optics: 1 – optical single cylinder engine, 2 – beam splitter, 3 – high-speed video camera for combustion visualization, 4 – focal lens, 5 – reflecting diffraction grating, 6 – image intensifier, 7 – high-speed camera for the emission spectrum

A.2. Methane Number calculation methodology for gaseous fuels

The gas fuel or gas fuel mixture composition was simplified into an inert-free mixture and it was sub-divided into a number of partial ternary mixtures (Methane

– Ethane – Butane; Propane – Ethane – Butane; Hydrogen – Propane – Propylene and etc.).

The number and particular partial ternary mixtures were chosen by available ternary systems in a given order according to the standard. Selection was stopped when all compounds were contained in at least two ternary systems. Priority was given to ternary systems that had all three components in a simplified mixture. Also the choice of ternary system was given, which had a highest fitness W_j value:

$$W_j = \sum_{i=1}^{i=n_m} \frac{V_{i,\min}\left(100\left(V_{\max_{i,j}} + 15\right)\right)}{V_{sum_i}}. \tag{A.1}$$

Here n_m – the number of components in a simplified mixture; V_i – the volume fraction of component *i* in a simplified mixture; $V_{max_{i,j}}$ – the maximum content of component *i* for the range of applicability; V_{sum_i} – the sum of all maximum contents of component *i* for the range of applicability of all systems.

$$V_{sum} = \sum_{i=1}^{j=18} \min\left(100, \left(V_{\max_{i,j}} + 15\right)\right). \tag{A.2}$$

The MN of each partial mixture was calculated from the general formula:

$$MN_t = \sum_{i=0}^{i=7} \sum_{j=0}^{j=6} \left(a_{i,j} x^i y^j\right). \tag{A.3}$$

Here *x* and *i* – the volume fractions of the first and second component in partial ternary mixture; $a_{i,j}$ – coefficient values of partial ternary systems which is given by EN standard.

The composition and fraction of the selected partial mixtures were adjusted iteratively in order to minimize the difference between the methane numbers of each partial mixture. The iterative optimization of MN calculation was done using *Microsoft Office* additional software package *Solver*. The calculations were done according Generalized Reduced Gradient (GRG) method, where optimized objects are difference of two MN values of different ternary mixtures which are written as functions:

$$MN_{\max} - MN_{\min}; \tag{A.4}$$

$$f_n\left(x_1, x_2, ..., x_n\right) - f_k\left(x_1, x_2, ..., x_n\right). \tag{A.5}$$

The changeable variables are volume fractions of any component $x_1, x_2, \ldots, x_n$ in any chosen ternary mixture m_k with a boundary which includes that sum of all ternary mixture volume fractions has to be 1:

$$m_k\left(x_1\right) + m_k\left(x_2\right) + ... + m_k\left(x_n\right) = 1; \tag{A.6}$$

$$k = 1, 2, ..., l;\ n = 1, 2, ..., p .$$

Also side constrains were applied. The sum of all ternary mixtures percentages cannot exceed 100%:

$$m_1(x_1, x_2, ..., x_n) + m_2(x_1, x_2, ..., x_n) + ... + m_k(x_1, x_2, ..., x_n) = 100 ; \quad \text{(A.7)}$$

$$k = 1, 2, ..., l .$$

The MN' of the simplified mixture is determined from the weighted average of the methane number of the selected partial mixtures.

$$MN' = \sum_{t=1}^{t=N_{sys}} (MN_t \cdot F_t) . \quad \text{(A.8)}$$

Here MN' – the methane number of the simplified mixture; MN_t – the methane number of a partial mixture t; F_t – the fraction of the partial mixture t; N_{sys} – the number of selected ternary systems.

The final MN of gaseous fuel is calculated by correction of a simplified mixture MN' when the presence of inert gases in the original fuel gas is included.

$$MN = MN' + MN_{inerts} - MN_{methane} . \quad \text{(A.9)}$$

A.3. Fuel mass distribution in different fuel mixtures

First experimental studies were performed with a 4 cylinder SI *HR16DE* engine fuelled with petrol and petrol with additional feeds of biogas. Such system worked as dual fuel system. Different petrol and 20 *l*/min. (*P* + *Bio* 20), 25 *l*/min. (*P* + *Bio* 25) and 30 *l*/min. (*P* + *Bio* 30) of biogas additive were tested. Petrol and biogas were injected into air intake manifold before the intake valves.

Engine throttle was opened at 15% during the study, which had a regular cylinder refilling ($\eta_v \approx 0.24$), that means that the engine regularly received ~ 40.7 m^3/h air or air / biogas mixture.

The CO_2 gas content in the biogas / air fuel mixture increased by ~ 1.85%, ~ 2.37% and ~ 2.74% (according to volume), when the amount of injected biogas (20 *l*/min., 25 *l*/min. and 30 *l*/min.) was changed, respectively. The methane element content in the gas mixture also increased by ~ 1.25%, ~ 1.60% and ~ 1.85%, respectively. Therefore the amount of supplied air to the engine decreased. However, the most important indicator is the distribution of different fuels content by mass. Fig. A.3.1 presents biogas and petrol content by mass in fuel depending on different amounts of additional biogas gas supply.

Depending on increasing amount of injected biogas fuel, the content of petrol mass in the fuel decreased from 100% up to ~ 66.01%, ~ 58.10%, and ~ 52.99% and the biogas content increased by ~ 33.99%, ~ 41.90% and ~ 47.01%.

During primary theoretical investigation of H_2 impact on the engine indicators, it was also determined that the intake air volume is about 40.70 m^3/h when the engine was running on petrol (n = 2000 rpm, throttle 15%, Θ = 18 CAD bTDC and $\lambda = 1$). It was also assumed that this intake gas volume remains constant when the engine intakes air / hydrogen gas mixture: $V = V_{air} + V_{H2} = const. = 40.70\ m^3/h$.

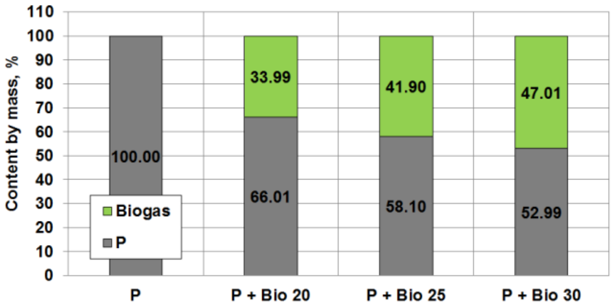

Fig. A.3.1. Content by mass of different fuels (biogas (*Bio*), petrol (*P*)) depending on different fuel supply amounts

Assuming theoretically, as 10% H_2 is supplied to air, it makes $V_{H2} = 4.07\ m^3/h$, and 15% H_2 hydrogen will take $V_{H2} = 6.10\ m^3/h$, respectively, therefore, intake air quantity will decrease down to $V_{air} = 36.64\ m^3/h$ and $V_{air} = 34.60\ m^3/h$, respectively. In this case, the engine control unit will decrease injected *P* fuel mass. While leaning the mixture from $\lambda = 0.9$ to $\lambda = 1.6$, the air quantity is getting higher (according to the determined air excess coefficient) and the injected H_2 mass is increasing also, but the mass of *P* fuel is reducing. The content by mass of injected *P* and H_2 fuel is calculated and presented in Fig. A.3.2. While leaning the mixture within the set limits at constant H_2 supply and as petrol quantity decreases (Fig. A.3.2), hydrogen mass concentration grows from ~ 12% to ~ 24% for *P* + 10% H_2 fuel mixture and from ~ 21 % to ~ 47% for *P* + 15% H_2 fuel mixture.

Figure A.6 represent the dependence of H_2 addition content by mass in CNG fuel when the CNG / H_2 fuel mixtures were mixed according to the volume fractions.

The lowest addition of 10% H_2 by volume gives just 1.29% according by mass if compared with CNG fuel amount. The H_2 increase up to 90% by volume in the fuel mixture showed that the content of H_2 by mass increased up to 53.08% which is more than a half of CNG fuel.

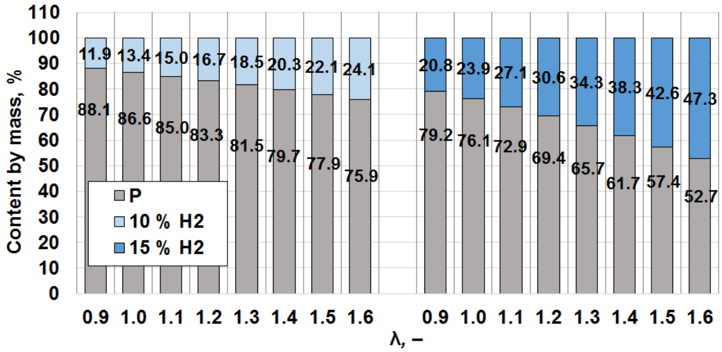

a) b)

Fig. A.3.2. Dependence of H_2 mass concentration in fuel mixture on different petrol and hydrogen fuel mixtures and air / fuel ratios: a) 10% hydrogen addition, b) 15% hydrogen addition

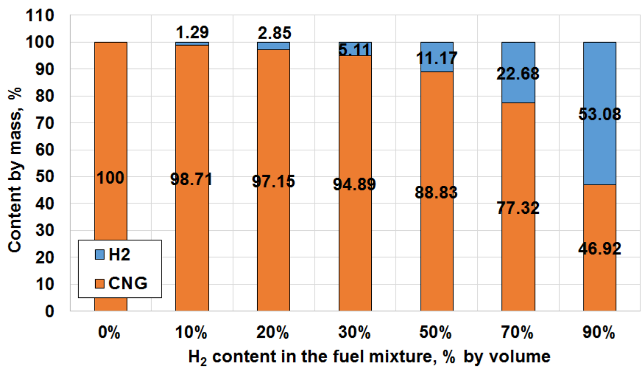

Fig. A.3.3. Dependence of H_2 mass concentrations on the natural gas and H_2 fuel mixtures when the fuel mixture is prepared according to the volume percentage

A.4. *AVL BOOST* simulation methodology

Fig. A.4.1 shows the energy balance of the cylinder and the variables which are included in calculations.

Mentioned thermodynamics law shows that the internal energy in the cylinder is equal to the sum of the piston work, fuel heat input, wall heat losses and the enthalpy flow due to blow-by.

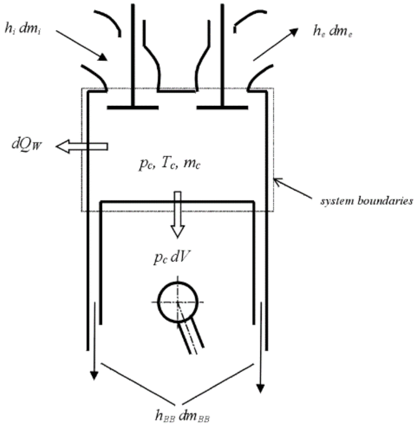

Fig. A.4.1. Schematics of energy balance in cylinder (*AVL BOOST* Theory 2011)

The heat transfer in engine and engine parts (like cylinder head, piston, cylinder liner) is calculated using formula:

$$Q_{wi} = A_i \cdot \alpha_w \cdot (T_c - T_{wi}) \cdot \qquad \text{(A.10)}$$

Here Q_{wi} – wall heat flow (cylinder head, piston, liner); A_i – surface area (cylinder head, piston, liner); α_w – heat transfer coefficient; T_c – gas temperature in the cylinder; T_{wi} – wall temperature (cylinder head, piston, liner).

The heat transfer coefficient was used to calculate using Woschni model:

$$a_w = 130 \cdot D^{-0.2} \cdot p_c^{0.8} \cdot T_c^{-0.53} \cdot \left[C_1 \cdot c_m + C_2 \cdot \frac{V_D \cdot T_{c,1}}{p_{c,1} \cdot V_{c,1}} \cdot \left(p_c - p_{c,o} \right) \right]^{0.8} . \qquad \text{(A.11)}$$

Here C_1 = 2.28 + 0.308 $\cdot$ c_u / c_m; C_2 = 0.00324 for DI engines; C_2 = 0.00622 for IDI engines; D – cylinder bore; c_m – mean piston speed; c_u – circumferential velocity; V_D – displacement per cylinder; $p_{c,o}$ – cylinder pressure of the motored engine, bar; $T_{c,1}$ – temperature in the cylinder at intake valve closing (IVC); $p_{c,1}$ – pressure in the cylinder at IVC.

A.5. Methodology for errors of calculated parameters

For the uncertainty calculations $u_c(f)$ it is accepted that M_e uncertainty $u_{Me}(x_i)$ is calculated according to formula (2.35) and the fuel consumption $u_{Bd}(x_i)$ uncertainty is calculated according to rectangular distribution with parameter a_d = 0.10 % = 0.001B_d according to formula (2.32):

$$u_{Bd}\left(x_i\right)=\frac{0.001\cdot B_d}{\sqrt{3}}\approx 0.00041\cdot B_d\ =4.1\cdot 10^{-4}\cdot B_d\,; \tag{A.12}$$

$u_{Me}(x_i)$ and $u_{Bd}(x_i)$ uncertainties depend on sample. For each sample different $u_{Me}(x_i)$ and $u_{Bd}(x_i)$ evaluations will be get. Though from all studied samples it is possible to choose highest $u_{Me}(x_i)$ and $u_{Bd}(x_i)$ values with which it is possible to calculate indirect measured value $u_c(f\,)$ standard uncertainty higher boundary.

After calculations it was determined that highest M_e uncertainty $max\{u_{upp,Me,j}\} = 2.358$ Nm. Highest B_d value $max\{B_{d,j}\} = 2628$ g/h. Then $max(u_{Bd}\} = 4.1\cdot 10^{-4}B_d = 4.1\cdot 10^{-4}\cdot 2628 = 1.08$ g/h.

(2.31) formula $\partial f/\partial x_i$ is partial derivative of a function $f\,(x_i)$ in respect of x_i variable. Otherwise $\partial f/\partial x_i$ is called sensitivity coefficient and is marked as c_i. $c_i=\partial f_i/\partial x_i$ expression can be found by differentiation of M_e and B_d expressions in (2.27), (2.28) and (2.29):

$$c_{P_e}=\frac{\partial P_e}{\partial M_e}=\frac{\partial}{\partial M_e}=\frac{M_e n_e}{9549}=\frac{n_e}{9549}; \tag{A.13}$$

$$\begin{aligned} c_{BSFC,1}&=\frac{\partial BSFC}{\partial B_d}=\frac{\partial}{\partial B_d}\frac{B_d\,9549}{M_e n_e}=\frac{9549}{M_e n_e};\\ c_{BSFC,2}&=\frac{\partial BSFC}{\partial M_e}=\frac{\partial}{\partial M_e}\frac{B_d\,9549}{M_e n_e}=\frac{B_d\,9549}{M_e^2 n_e}; \end{aligned} \tag{A.14}$$

$$\begin{aligned} c_{\eta e,1}&=\frac{\partial \eta_e}{\partial M_e}=\frac{\partial}{\partial M_e}\frac{3600 M_e n_e}{9549 B_d LHV}=\frac{3600 n_e}{9549 B_d LHV};\\ c_{\eta e,2}&=\frac{\partial \eta_e}{\partial B_d}=\frac{\partial}{\partial B_d}\frac{3600 M_e n_e}{9549 B_d LHV}=\frac{3600 M_e n_e}{9549 B_d^2 LHV}. \end{aligned} \tag{A.15}$$

Then the final uncertainty formulas will be (according to (2.30) and (2.31) formulas):

- Engine power P_e, kW

$$u_c\left(P_e\right)=\sqrt{c_{P_e}{}^2 u_{M_e}{}^2}\,. \tag{A.16}$$

- Brake specific fuel consumption BSFC, g/kWh

$$u_c\left(BSFC\right)=\sqrt{c_{BSFC,1}{}^2 u_{Bd}{}^2+c_{BSFC,2}{}^2 u_{M_e}{}^2}\,. \tag{A.17}$$

- Engine thermal efficiency η_e

$$u_c\left(\eta_e\right)=\sqrt{c_{\eta e,1}{}^2 u_{M_e}{}^2+c_{\eta e,2}{}^2 u_{B_d}{}^2}\,. \tag{A.18}$$

Here the specific case calculations from CNG / H_2 experimental tests are presented when CNG fuel at $\lambda = 1.4$ case was measured: $M_e = 42$ Nm, $n_e = 2005$ rpm, $B_d = 2016$ g/h and LHV = 50.4 MJ/kg, accordingly calculated values are $P_e = 9.1$ kW, $BSFC = 221.538$ g/kWh and $\eta_e = 0.29422$.

Calculated values were input into (A.16) – (A.18) formulas with taken $max\{u_{upp,Me,j}\} = 2.358$ Nm and $max(u_{Bd}\} = 1.08$ g/h values. The uncertainty values are:

1. $u_c(P_e) = 0.4951$, ratio $U_c(P_e)/P_e = 5.441\%$;
2. $u_c(BSFC) = 12.84$, ratio $U_c(BSFC)/BSFC = 5.794\%$;
3. $u_c(\eta_e) = 5.983 \cdot 10^{-3}$, ratio $U_c(\eta_e)/\eta_e = 2.034\%$.